Korean J. Chem. Eng., 33(3), 976-985 (2016)
DOI: 10.1007/s11814-015-0182-z

pISSN: 0256-1115
eISSN: 1975-7220

Adsorption properties of silica surface-grafted with a salicylhydroxamic acid-functionalized polymer toward lead ions

Ruixin Wang†, Meina Xie, Hongjing Wang, Xiaohui Shi, and Caiping Lei

School of Chemical and Environmental Engineering, North University of China, Taiyuan 030051, China
(*Received 16 March 2015 • accepted 28 August 2015*)

Abstract−Salicylhydroxamic acid (SHA), functionalized composite chelating adsorbing material SHA-PHEMA/SiO_2, was prepared through the nucleophilic substitution reaction of 5-chloromethyl-salicylhydroxamic acid with poly (2-hydroethyl methacrylate) (PHEMA) modified silica gel particles PHEMA/SiO_2. The SHA-PHEMA/SiO_2 composites were characterized by FT-IR, scanning electron microscopy, X-ray photoelectron spectroscopy and nitrogen absorption. The adsorption behavior, adsorption thermodynamic, and adsorption mechanism of SHA-PHEMA/SiO_2 for Pb^{2+} ions were studied, and the pH value of the medium on the adsorption property and chelating adsorption ability of SHA-PHEMA/SiO_2 for Pb^{2+} ions was also investigated. The experimental results show that SHA-PHEMA/SiO_2 possesses strong chelating adsorption ability for Pb^{2+} ions, and the adsorption capacity for Pb^{2+} ions at 308K reached 57 mg/g. The adsorption process is a chemical adsorption process driven by entropy, and the adsorption capacity increases with rising temperature. In pH range that can inhibit the hydrolysis of heavy metal ions, increasing the pH value of the medium strengthens the adsorption ability of SHA-PHEMA/SiO_2 toward Pb^{2+} ions. The adsorption behavior is monomolecular and follows Langmuir isotherm. The adsorption capacity is almost the same after ten consecutive adsorption-desorption experiments of SHA-PHEMA/SiO_2 for Pb^{2+} ions, indicating that SHA-PHEMA/SiO_2 has excellent elution property and reusability.

Keywords: Salicylhydroxamic Acid, Poly (2-Hydroethyl Methacrylate), Silica Gel, Chelation, Lead Ions

INTRODUCTION

Chelating resin is a commonly used adsorbent [1-4]. Various functional groups can chelate with metal ions, such as 8-hydroxyquinoline, imide acid, Schiff base, salicylic acid, and amidoxime on the resin matrix. They have been widely used in analysis and detection, concentration and enrichment, separation and removal of metal ions, and so on [5-7]. The material is not only easy to handle but is relatively affordable and effective in removing heavy metal ions, particularly at low concentration. In addition to the chelating resin, composite chelating adsorbent materials also attract research attention [8-12]. Composite chelating adsorption material is mainly composed of inorganic particles (such as silica gel, montmorillonite, and hydroxylapatite) and chelating reagents, including the small molecule chelating reagent, and chelating group-functionalized polymer. The aforementioned composite chelating adsorption material composed of chelating group-functionalized polymer and inorganic particles has a strong chelating adsorption property because of the high density of chelating groups and the high specific surface for the composite chelating adsorption material. Furthermore, this composite material exhibits the advantages of inorganic particles, such as good mechanical properties, satisfactory thermal stability, low cost, and so on. Therefore, these materials have been extensively studied to remove heavy metal ions from industrial wastewater [13-16].

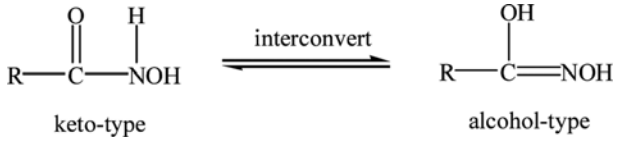

Fig. 1. Isomers of hydroxamic acid.

Hydroxamic acid, also called hydroxyl oxime acid, results from the simultaneous existence of two isomers of keto-type and alcohol-type, as shown in Fig. 1. Hydroxamic acid is a kind of important metal chelating agent [17,18]. The nitrogen and oxygen atoms with lone pair electrons exist simultaneously in hydroxamic acid molecules and are close to each other. Hydroxamic acid can chelate with metal ions easily to form a stable four- or five-numbered ring, as shown in Fig. 2. Hydroxamic acid has been widely applied in mineral flotation, such as earth ore, bauxite, wolframite, and scheelite [19-22]. Additionally, chelates of hydroxamic acid with metal ions can also be used as monooxygenase catalyst [23,24], simulated iron

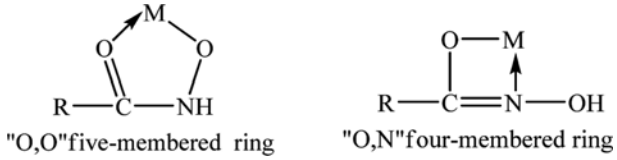

Fig. 2. Chelation between hydroxamic acid and metal ions.

†To whom correspondence should be addressed.
E-mail: wrx0212@126.com

carrier protein [25], anticancer agents [26], and so on. However, hydroxamic acid is mostly used in the form of free molecule in the preceding applications, which shows not only poor physical and chemical stability but also difficulty in separation, recovery, and reuse.

In this study, the chemical structure of the composite adsorbent was well designed. First, poly (2-hydroethyl methacrylate) (PHEMA) was grafted onto the silica gel surface to obtain PHEMA/SiO_2 composite material, which possesses superior chemical and mechanical properties and strong hydrophilicity for good water solubility of PHEMA. Then, the chloromethylation reaction of salicylhydroxamic acid (SHA) was performed using 1-4-bis (chloromethoxy) butane (BCMB) as chloromethylation reagent to obtain 5-chloromethyl-salicylhydroxamic acid (CMSHA). Finally, CMSHA was bonded into PHEMA/SiO_2 via a polymer reaction between them to obtain the salicylhydroxamic acid-functionalized composite adsorption material SHA-PHEMA/SiO_2. The kinetic and thermodynamic properties of the adsorption, as well as the adsorption mechanism for metal ions, were mainly investigated. The results show that SHA-PHEMA/SiO_2 presents excellent adsorption abilities and reusability.

EXPERIMENTS

1. Materials

The materials used in the experiments include silica (120-160 mesh, approximately 125 μm diameter, Ocean Chemical Limited Company, Shandong, China), agent grade 2-hydroxyethyl methylacrylate (HEMA) (Tianjin Chemical Reagent Research Institute, China), analytical grade, vacuum distillation purification before using γ-aminopropyl trimethoxysilane (AMPS) (Yongchang Chemical Limited Company, Nanking, China), analytical grade, salicylhydroxamic acid (SHA) (Henan Xinxiang Tianfeng Fine Chemical Company, China), and analytical grade 1, 4-dichloro methoxybutane (BCMB), homemade according to the reference [27]. All other chemicals used in the experiment were of commercial analytical grade and purchased from Chinese companies.

2. Preparation and Characterization of Functionalized Composite Chelating Material SHA-PHEMA/SiO_2

2-1. Preparation of 5-Chloromethyl-Salicylhydroxamic Acid (CMSHA) [28]

First, 10 g of SHA was added into a four-necked flask with 100 mL of N, N-dimethylformamide (DMF) in which SHA was dissolved completely. Subsequently, 21 mL of BCMB and 1.2 mL of $SnCl_4$ were added slowly into the solution in an ice-water bath. The chloromethylation reaction was conducted at 0 °C for 13 h. Then, the pH value of the content was adjusted to 6-7 and left overnight to obtain white precipitation. Finally, the precipitation was washed with acetone repeatedly, and recrystallization was conducted to purify the product to obtain CMSHA. The chemical structure of CMSHA was determined by IR spectrum using KBr pellet method.

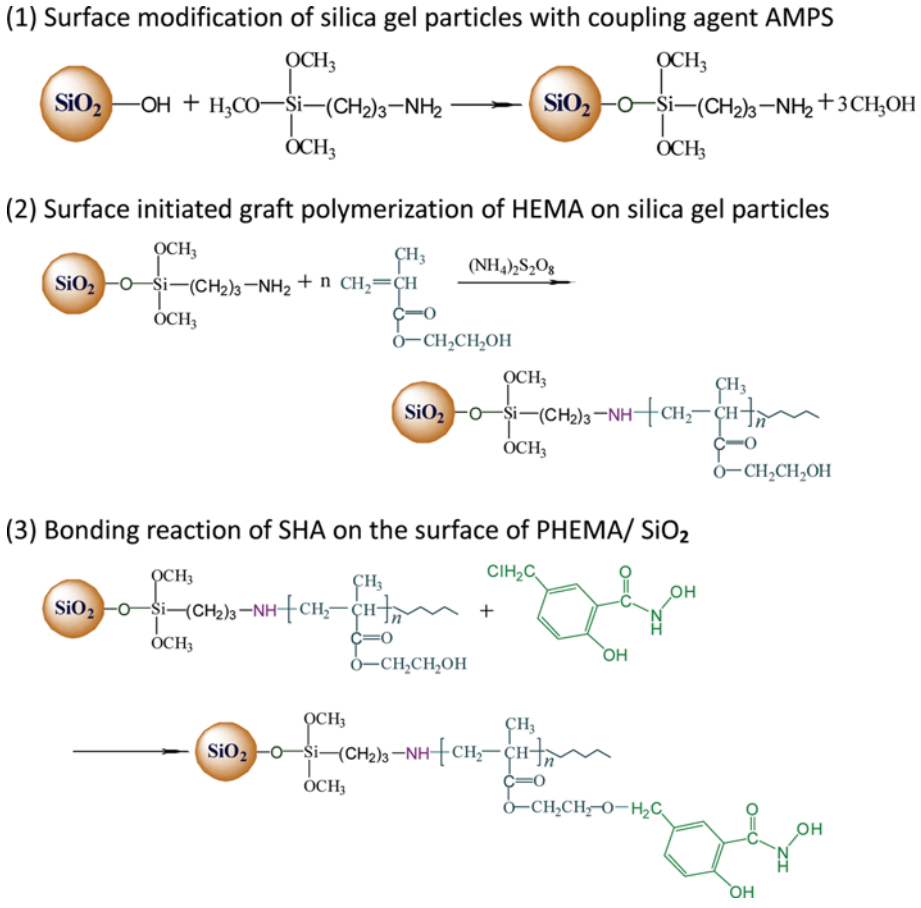

Scheme 1. Schematic expression of preparation process of SHA-PHEMA/SiO_2.

2-2. Preparation of SHA-PHEMA/SiO_2

First, 10 g of silica gel particles activated with methane sulfoacid and 10 ml of coupling agent AMPS were added into 100 ml of water. The contents were stirred for 24 h at 50 °C to obtain the surface-modified particles AMPS-SiO_2. Second, 1 g of AMPS-SiO_2 and 5 mL HEMA were added into 100 mL of a mixed solution of DMF and water (V : V=1 : 1). Graft polymerization was performed by initiating $(NH_4)_2S_2O_8$ (0.6 wt% of monomer) under N_2 atmosphere at 70 °C for 24 h. The product particles were washed with distilled water and methyl alcohol repeatedly to remove the polymers attached physically to the particles and then dried under vacuum, which resulted in the grafted particles of PHEMA/SiO_2 [29]. Subsequently, 0.5 g of PHEMA/SiO_2 and 2.06 g of CMSHA were added to 20 mL of dimethylsulfoxide with 3.48 g of $NaCO_3$ as acid-binding agent. Nucleophile substitution reaction between the hydroxyl group of PHEMA and the chloromethyl of CMSHA occurred under N_2 atmosphere at 100 °C for 10 h. Finally, the composite adsorbent SHA-PHEMA/SiO_2 was prepared. The preparation process of SHA-PHEMA/SiO_2 is shown as Scheme 1. The bonding rate of SHA units on the adsorbent SHA-PHEMA/SiO_2 was measured by thermogravimetric analyzer (TGA, Netzsch Group STA449, Germany). The SHA-PHEMA/SiO_2 used in this study had a bonding rate of 31.4%.

3. Characterization

The chemical structure of SHA-PHEMA/SiO_2 was characterized by a Fourier transform infrared spectrometer (FT-IR, Perkin-Elmer Company 1700, US). The morphology of SHA-PHEMA/SiO_2 was observed by scanning electron microscopy (SEM, JEOL JSM-6700, Japan). The chemical states and structure of the lead adsorbed by SHA-PHEMA/SiO_2 surface were studied by X-ray photoelectron spectroscopy (XPS, Kratos axis ultra dld, Japan). The adsorption-desorption isotherm of N2 at 77 K was measured with an automated surface area and pore size analyzer (Quantachrome Quadrasorb SI, USA) to evaluate its surface area. The specific surface area and the pore size were determined using BET equation and BJH method, respectively. The charging of SHA-PHEMA/SiO_2 surface was tested by Zeta potential and particle size analyzer (Brookhaven Zetaplus, USA).

4. Static Adsorbing Experiments

4-1. Adsorption Kinetics Experiments

A solution consisting of 0.03 g of SHA-PHEMA/SiO_2 and 30 mL of Pb^{2+} water solution with an initial concentration (C_0) (pH of 6) was placed into numerous conical flasks with plugs. The conical flasks were agitated in a shaker at 25 °C. Then, the concentrations (C_t, mg/L) of Pb^{2+} in the supernatants at different time (t) points were determined by EDTA complexometric titration. The corresponding adsorption amounts (Q, mg/g) were calculated according to Eq. (1), and the adsorption kinetic curve was plotted.

$$Q = \frac{V(C_0 - C_t)}{m} \quad (1)$$

where V (L) is the volume of the metal ion solution and m (g) is the weight of the adsorbent SHA-PHEMA/SiO_2.

4-2. Isothermal Adsorption Experiments

Thirty (30) mL of aqueous solution of Pb^{2+} ions with different initial concentrations (C_0=100, 200, 300, ····, 800 mg/L) and the same pH of 6 was placed into numerous conical flasks with plug, and approximately 0.03 g of SHA-PHEMA/SiO_2 was introduced into these solutions. These mixtures were shaken in a constant temperature oscillator for 2 h to reach equilibrium. The equilibrium concentration (C_e, mg/L) of metal ions in the supernatant was determined by EDTA complexometric titration, and the equilibrium adsorption amount (Q_e, mg/g) was calculated according to Eq. (2). Then, the adsorption isotherm of SHA-PHEMA/SiO_2 for Cu^{2+} ion was obtained.

$$Q_e = \frac{V(C_0 - C_e)}{m} \quad (2)$$

where V (L) is the volume of the metal ion solutions and m (g) is the weight of the adsorbent SHA-PHEMA/SiO_2.

To evaluate the effect of the temperature and pH value on the adsorption property of SHA-PHEMA/SiO_2 and to investigate in depth its adsorption mechanism and thermodynamics toward metal ions, the isothermal adsorption experiments were conducted at different temperatures and pH values.

5. Dynamics Adsorption and Elution Experiments

A glass column with 8 mm diameter was filled with 1.12 g of SHA-PHEMA/SiO_2 and 2 mL of the bed volume (BV). At room temperature (23 °C), Pb^{2+} ion solution with concentration of 600 mg/L and pH 5.5 was allowed to flow gradually through the column at a rate of four bed volumes per hour (4 BV/h). Two BV of effluent were collected, and the concentration of Pb^{2+} ion was determined by EDTA complexometric titration. Then, the dynamic adsorption curve was plotted, and the leak adsorption amount and saturated adsorption capacity were also calculated.

Elution experiment was conducted using 0.1 mol/L of hydrochloric acid solution as eluting agent, and the flow rate of the eluting agent was controlled at 1 BV/h. The eluent with one BV was collected and the concentration of Pb^{2+} ion was determined. Then, the dynamic elution curve was plotted.

6. Repeated Use Experiment

Reusability is a highly important property for the effective adsorbent. Pb^{2+} ion saturately adsorbed on SHA-PHEMA/SiO_2 was desorbed in 0.1 mol/L of hydrochloric acid solution at 20 °C for 5 h. Pb^{2+} ion saturately adsorbed on SHA-PHEMA/SiO_2 could be desorbed completely using 0.1 mol/L of hydrochloric acid solution as the eluting agent. To test the reusability of SHA-PHEMA/SiO_2, the static adsorption-desorption experiments for Pb^{2+} ion were repeated consecutively ten times by using the same SHA-PHEMA/SiO_2.

RESULTS AND DISCUSSION

1. Characterization of Composite Material SHA-PHEMA/SiO_2

1-1. Infrared Spectra

Fig. 3 presents the IR spectra of the grafted particle PHEMA/SiO_2, functional particle SHA-PHEMA/SiO_2, and metal complex particle Pb^{2+}-SHA-PHEMA/SiO_2. Compared with the spectrum of PHEMA/SiO_2, three new characteristic absorption bands at 1,635 cm^{-1}, 1,559 cm^{-1}, and 1,535 cm^{-1} were exhibited in the spectrum of SHA-PHEMA/SiO_2. The absorption band at 1,635 cm^{-1} was the absorption band of carbonyl of SHA, and the absorption bands at 1,559 cm^{-1} and 1,535 cm^{-1} corresponded to the vibration of the ben-

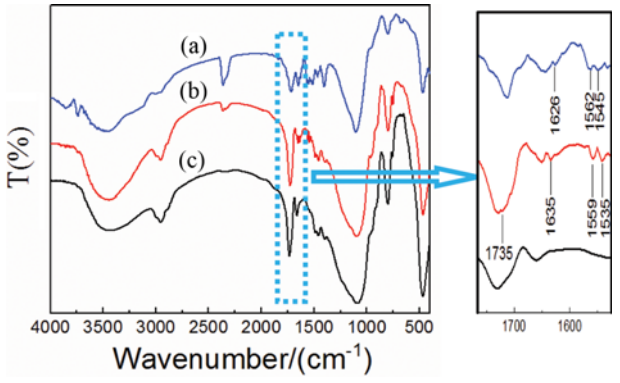

Fig. 3. FTIR spectra of (a) Pb^{2+}-SHA-PHEMA/SiO_2, (b) SHA-PHEMA/SiO_2 and (c) PHEMA/SiO_2.

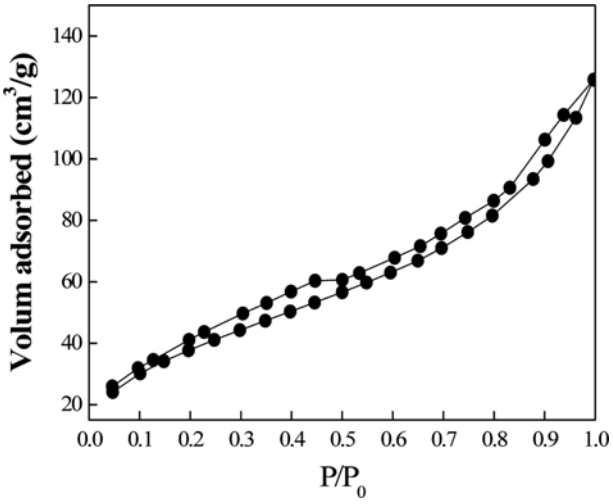

Fig. 5. N_2 adsorption isotherms of SHA-PHEMA/SiO_2 particles.

zene ring of SHA. These results imply that SHA had bonded onto the silica gel surface, gaining the composite adsorbing material SHA-PHEMA/SiO_2. In the spectrum of Pb^{2+}-SHA-PHEMA/SiO_2, the characteristic absorption band of carbonyl at 1,635 cm^{-1} shifted to the lower wave number of 1,626 cm^{-1}, indicating the formation of the coordination bond between C=O and Pb^{2+} ion.

1-2. Morphology of SHA-PHEMA/SiO_2 Particles

Fig. 4 gives the SEM micrographs of SiO_2 particles (a) and SHA-PHEMA/SiO_2 composite particles (b). It is obvious that the surface of SHA-PHEMA/SiO_2 composite particles was smoother than that of SiO_2 particles, resulting from the filling up and covering of the grafted polymer layer (SHA-PHEMA).

1-3. Porous Properties of SHA-PHEMA/SiO_2 Particles

The N_2 adsorption isotherm for SHA-PHEMA/SiO_2 is shown in Fig. 5. It is clear that SHA-PHEMA/SiO_2 exhibited a typical type II isotherm. The major uptake occurred at relative high pressures, indicating that SHA-PHEMA/SiO_2 possessed a number of mesoporous.

BET surface area, pore volume, and average pore size of SHA-PHEMA/SiO_2 composite particles and SiO_2 particles are summarized in Table 1. The results show that after graft-polymerization, the surface area (S_{BET}), total pore volume (V_{tot}) and the average pore size (D) of SHA-PHEMA/SiO_2 decreased largely compared with

Table 1. Surface area, pore volume and average pore size of SiO_2 and SHA-PHEMA/SiO_2

Samples	S_{BET} (m^2/g)	D (nm)	V_{tot} (cm^3/g)
SiO_2	350	6	1.0
SHA-PHEMA/SiO_2	142.697	3.053	0.148

the pure SiO_2, indicating that the grafted polymer could block some of mesoporous of SiO_2.

1-4. X-ray Photoelectron Spectroscopy of Lead-loaded Pb^{2+}-SHA-PHEMA/SiO_2

The wide scan and high resolution XPS spectra of the lead-loaded Pb^{2+}-SHA-PHEMA/SiO_2 are shown in Fig. 6. The high resolution XPS spectrum (Fig. 6(B)) shows two clear peaks around binding energies (BE) of 138.7 eV and 143.5 eV corresponding to $Pb4f_{7/2}$ and $Pb4f_{5/2}$, respectively, indicating the lead uptake on the SHA-PHEMA/SiO_2 particles.

2. Kinetic Adsorption Curve

Fig. 7 provides the adsorption kinetics curves of the composite

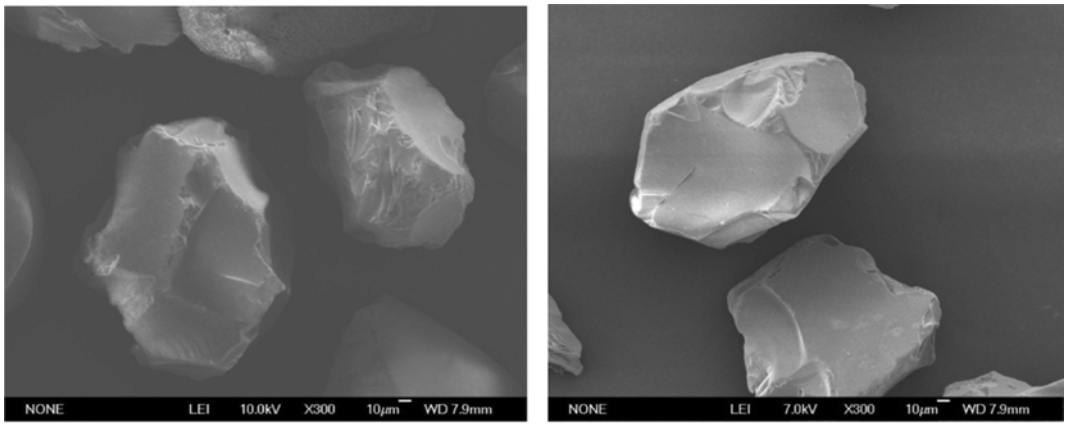

(a) (b)

Fig. 4. SEM images of SiO_2 and SHA-PHEMA/SiO_2 particles.

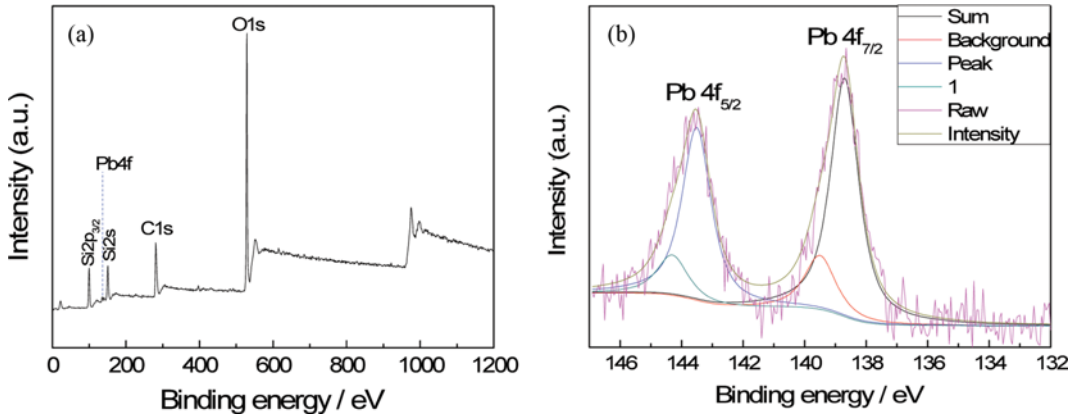

Fig. 6. Wide scan (a) and high resolution (b) XPS spectra of lead-loaded Pb^{2+}-SHA-PHEMA/SiO_2.

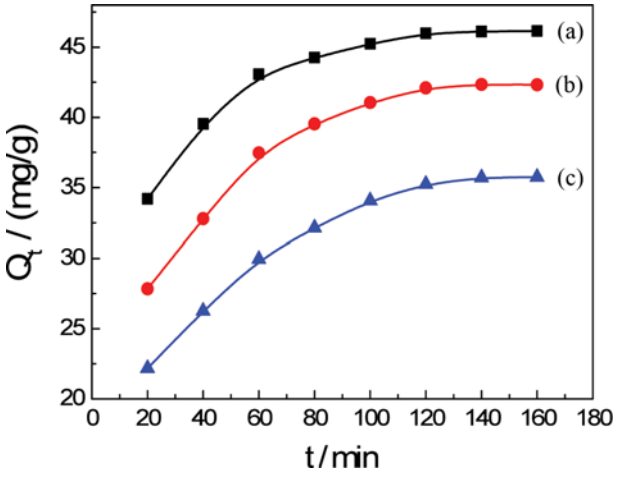

Fig. 7. Adsorption dynamics curve of SHA-PHEMA/SiO_2 toward Pb^{2+} ions (T=25 °C; pH=6; C_0: (a) 600 mg/L, (b) 400 mg/L, (c) 200 mg/L).

adsorption material SHA-PHEMA/SiO_2 toward Pb^{2+} ions. The figure indicates that all the adsorptions of SHA-PHEMA/SiO_2 toward Pb^{2+} ions with different concentrations almost can reach equilibrium at 2 h, displaying a faster rate. This faster adsorption rate may be due to the following reasons: (1) the chelating interaction between salicylhydroxamic groups on the surface of SHA-PHEMA/SiO_2 and metal ions, and (2) the good hydrophilicity of PHEMA of SHA-PHEMA/SiO_2 stretched the polymer chains better in water, such that metal ions could easily spread to the silica surface and chelate with hydroxamic groups.

Two kinetic models, pseudo-first-order and pseudo-second-order, were applied to fit the experimental data and analyze the adsorption mechanism of Pb^{2+} ions on SHA-PHEMA/SiO_2, as shown in Fig. 8. The fitting parameters are presented in Table 2.

The pseudo-first-order kinetic model [30] is expressed by the following formula:

$$\ln(Q_e - Q_t) = \ln Q_e - k_1 t \tag{3}$$

The pseudo-second-order kinetic model [31] is expressed by formula (4).

$$\frac{t}{Q_t} = \frac{1}{k_2 Q_e^2} + \frac{t}{Q_e} \tag{4}$$

where k_1 (min^{-1}) and k_2 (g/(mg·min)) are the adsorption rate con-

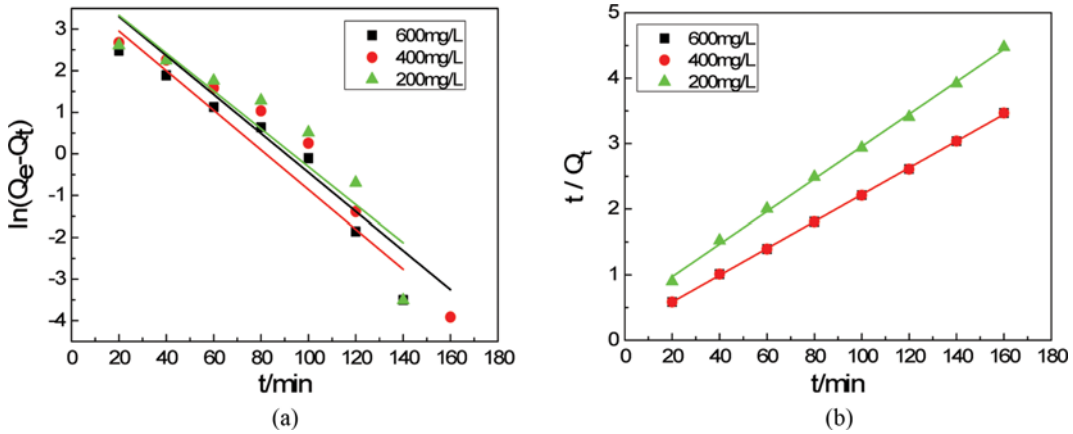

Fig. 8. Pseudo-first-order (a) and pseudo-second-order (b) adsorption kinetic equations of Pb^{2+} (T=25 °C; pH=6; C_0: (a) 600 mg/L, (b) 400 mg/L, (c) 200 mg/L).

Table 2. Kinetic parameters for adsorption rate expressions

$C_0/(mg \cdot L^{-1})$	Pseudo-first-order kinetic equations		Pseudo-second-order kinetic equations	
	k_1/min^{-1}	R^2	$k_2/(g \cdot (mg \cdot min)^{-1})$	R^2
600	0.0476	0.9269	0.0024	0.9999
400	0.0468	0.9389	0.0032	0.9998
200	0.0455	0.8261	0.0017	0.9983

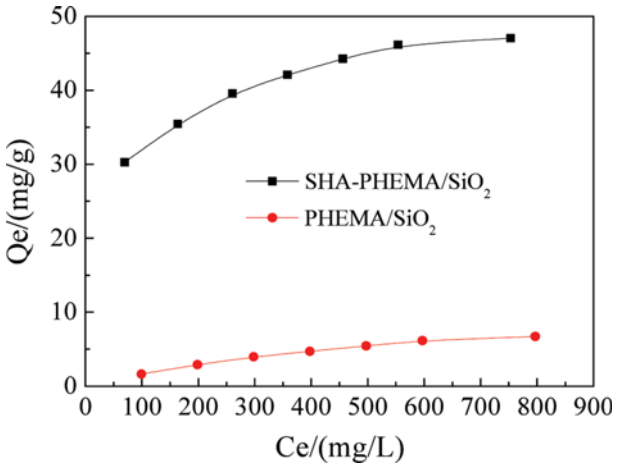

Fig. 9. Adsorption isotherms of SHA-PHEMA/SiO_2 and PHEMA/SiO_2 for Pb^{2+} ions (T=25 °C; t=2 h; pH=6).

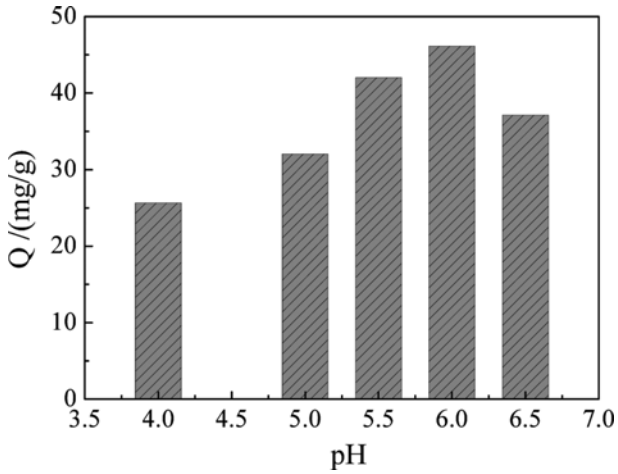

Fig. 10. Effect of pH value on adsorption property of SHA-PHEMA/SiO_2 (T=25 °C; t=2 h; C_0=600 mg/L).

stants of the first- and second-order kinetic models, respectively. Q_e and Q_t, in mg/g, represent the equilibrium adsorption uptake and adsorption uptake at time t, respectively.

Fig. 8(a) and (b) and Table 2 show that all the correlation coefficients ($R^2 \geq 0.9983$) of the pseudo-second-order kinetic model are higher than those of the pseudo-first-order kinetic model ($R^2 < 0.9400$), which implies that the pseudo-second-order kinetic model can describe the adsorption process better. The adsorption processes contained in the pseudo-second-order kinetic model, such as external liquid film diffusion, surface adsorption, and intraparticle diffusion, can reflect the adsorption mechanism of SHA-PHEMA/SiO_2 toward Pb^{2+} ions more accurately.

3. Adsorption Isotherm

Fig. 9 provides the adsorption isotherms of SHA-PHEMA/SiO_2 and PHEMA/SiO_2 for Pb^{2+} ion. The figure indicates that the adsorption ability of PHEMA/SiO_2 for Pb^{2+} ion is extremely weak because no functional groups can interact with Pb^{2+} ion. However, the composite adsorption material SHA-PHEMA/SiO_2 exhibited strong adsorption ability for Pb^{2+} ion, which was different from the performance of PHEMA/SiO_2, and the saturated adsorption capacity obtained was up to 46.8 mg/g. Near nitrogen and oxygen atoms in hydroxamic acid groups were weak electron donors with lone pair electrons and could easily chelate with metal ions to form stable "O, N" four-numbered ring or "O, O" five-numbered ring with metal (as shown in Fig. 2). However, "O, O" five-numbered ring was formed mainly because this ring was more stable than the four-numbered ring [32]. Therefore, hydroxamic groups on the surface of SHA-PHEMA/SiO_2 show strong chelated ability toward metal ions, forming a stable five-numbered ring. Moreover, multiple ligands chelate would be formed because of the co-chelation of the adjacent hydroxamic groups on the surface of SHA-PHEMA/SiO_2. All these characteristics enable SHA-PHEMA/SiO_2 to show strong chelating adsorption ability for heavy metal ions.

4. Effect of pH Value on Adsorption Capacity of SHA-PHEMA/SiO_2

The saturated adsorption amount as a function of pH value is shown in Fig. 10 to display the effect of pH value on adsorption capacity clearly. The maximum adsorption capacity occurred at approximately pH≤6 as shown in Fig. 10. It was found in experiments that nearly no adsorption occurred at pH 1. The adsorption amount of SHA-PHEMA/SiO_2 for Pb^{2+} ion increased significantly with the increase of pH value. Nevertheless, the adsorption amount decreased as pH was over 6.

SHA is a weak diprotic acid with *pKa* of ~7.4 (hydroxamic acid proton) and 9.8 (phenolic proton). It is also a base with three protonation sites: carbonyl oxygen, N-hydroxy oxygen and phenolic oxygen. In highly acidic conditions, some of the base sites can be protonated, which prevents its combination with metal ions, resulting in the lower adsorption capacity of SHA-PHEMA/SiO_2 for Pb^{2+} ion in acid medium. To verify this effect, the zeta potential of SHA-PHEMA/SiO_2 fine particles was determined and shown in Fig. 11 under different pH. It can be seen that as pH is lower than 6.5, SHA-PHEMA/SiO_2 surface is positively charged, which keeps it away from Pb^{2+} ion for the electrostatic repulsion. And the zeta potential value decreases continuously with rise of pH, making SHA-PHEMA/SiO_2 combined with Pb^{2+} ion more easily to obtain the higher adsorption capacity. However, when pH is higher than 7.5, the SHA-PHEMA/SiO_2 surface is negatively charged, which makes

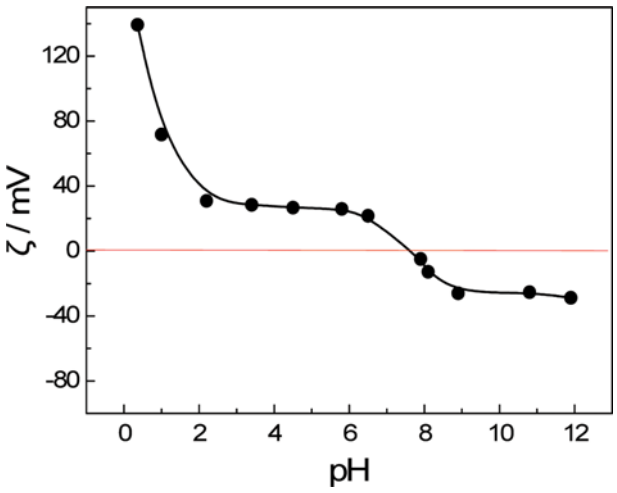

Fig. 11. Zeta potential of SHA-PHEMA/SiO_2 fine particles under different pH.

it more accessible to Pb^{2+} ion for the electrostatic attraction. So the adsorption capacity should be theoretically higher. But the heavy metal ions are well known to undergo hydrolysis under basic conditions (the first-order hydrolysis constant of Pb^{2+} ion was $K_1=6.3\times10^{-8}$) and white colloidal particles were generated, covering the surfaces of SHA-PHEMA/SiO_2 particles, such that the adsorption property was seriously impaired and the adsorption capacity declined. Therefore, SHA-PHEMA/SiO_2 could demonstrate the strong chelating adsorption ability for Pb^{2+} ion only when the pH value was moderate: pH=6.

5. Effect of Temperature on Adsorption Capacity of SHA-PHEMA/SiO_2 and Chelating Adsorption Thermodynamics

Adsorption isotherms at different temperatures are presented in Fig. 12. The adsorption capacity of Pb^{2+} ion increases with the rise in temperature. Physical adsorption is typically exothermic, and the adsorption amount reduces with the rising temperature. The adsorption of SHA-PHEMA/SiO_2 for Pb^{2+} ion is endothermic, which implies chemical adsorption. The chemical adsorption originated from the chelate of hydroxamic acid toward Pb^{2+} ions.

Langmuir isothermal adsorption equation is presented in Eq. (5), and the figure of C_e/Q_e versus C_e should be a straight line.

$$\frac{C_e}{Q_e}=\frac{C_e}{Q_m}+\frac{1}{bQ_m} \tag{5}$$

where C_e (mg/L) is the equilibrium concentration of Pb^{2+} ion. Q_e and Q_m, (mg/ g) are the equilibrium and saturated adsorption amounts of Pb^{2+} ion, respectively, and b is Langmuir constant.

Dubinin-Radushkevich (D-R) isothermal adsorption equation is presented in Eqs. (6), (7) and (8).

$$\ln Q_e=\ln Q_m-K'\varepsilon^2 \tag{6}$$

$$\varepsilon=RT\ln(1+1/C_e) \tag{7}$$

where C_e (mol/L) is the equilibrium concentration of Pb^{2+} ion. Q_e and Q_m, (mol/g) are the equilibrium and saturated adsorption amounts of Pb^{2+} ion, respectively. ε is the Polanyi activation energy. K′ is the constant related to adsorption energy.

The data in Fig. 12 were treated using Langmuir adsorption equation, and the four fitting lines were obtained as shown in Fig. 13. The linear dependences were all fine with correlation coefficients higher than 0.99 (see Table 3). In addition, the data in Fig. 12 were also treated using D-R equation, and the related parameters listed in Table 3. The correlation coefficients from D-R equation were lower than 0.99, and the calculated Q_m were far greater than that from

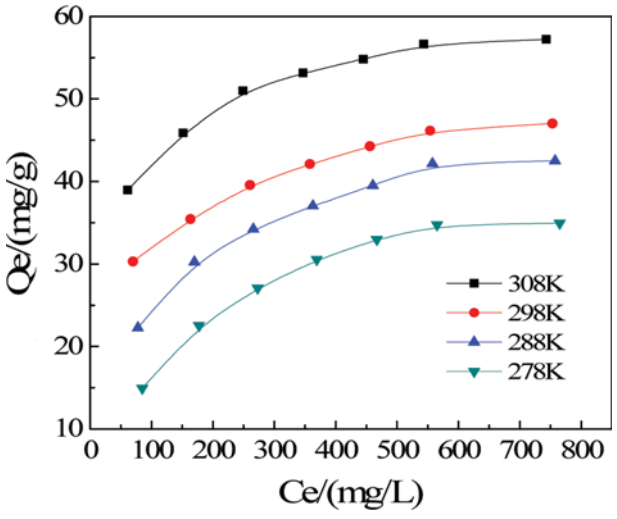

Fig. 12. Adsorption isotherms of SHA-PHEMA/SiO_2 for Pb^{2+} ion at different temperatures (pH=6; t=2 h).

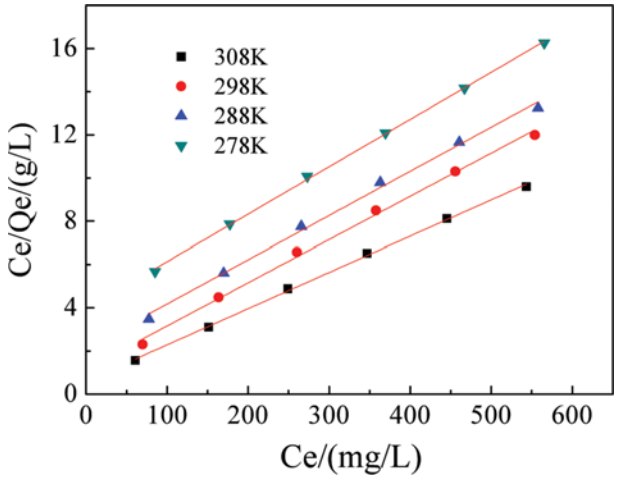

Fig. 13. Adsorption isotherms of SHA-PHEMA/SiO_2 for Pb^{2+} ion at different temperatures (pH=6; t=2 h).

Table 3. Related constants and linear regression coefficients of Langmuir fitting

T/K	Langmuir			D-R	
	Q_m/(mg/g)	b/(L/mg)	R^2	Q_m/(mmol/g)	R^2
278	45.66	0.0055	0.9993	0.4753	0.9682
288	49.02	0.0095	0.9953	0.4266	0.9838
298	50.00	0.0171	0.9961	0.3623	0.9919
308	59.52	0.0273	0.9988	0.4106	0.9878

experiment, indicating that the adsorption behavior of SHA-PHEMA/SiO_2 could not be described by the D-R equation, but conformed to the Langmuir model and was a monolayer adsorption process.

Langmuir constants at different temperatures could be calculated by means of the slopes and intercepts of four lines in Fig. 13 (see Table 3). For solid-liquid adsorption, a relationship existed between the Langmuir constant b and the adsorption equilibrium constant K as shown in Eq. (8) [33-35]. Thus, K can be obtained according to the following equation:

$$b=(K-1)\times M/\rho \quad (8)$$

where M and ρ are the molar mass and density of the solvent (water), respectively.

Van't Hoff equation, as shown in Eq. (9), revealed the relationship between the adsorption equilibrium constant K and temperature T. The adsorption enthalpy change ΔH can be calculated according to the slope of the straight line of lnK versus 1/T presented in Fig. 14, whereas Gibbs free energy change ΔG and entropy change ΔS can be obtained from thermodynamic Eqs. (10) and (11). The data of ΔH, ΔG, and ΔS are summarized in Table 4.

$$\ln K=-\frac{\Delta H}{R}\times\frac{1}{T}+C \quad (9)$$

$$\Delta G=-RT\ln K \quad (10)$$

$$\Delta G=\Delta H-T\Delta S \quad (11)$$

Table 4 reveals that (1) Gibbs free energy change ΔG is negative, which confirms that the chelating adsorption process of SHA-PHEMA/SiO_2 for Pb^{2+} ion is spontaneous; (2) adsorption enthalpy change ΔH is greater than zero, which indicates that the chelating adsorption is an endothermic as well as a chemical adsorption process; and (3) adsorption entropy change ΔS is greater than zero, which shows that the chelating adsorption is an entropy-increasing process. The preceding data and Eq. (11) indicated that the chelating adsorption process of SHA-PHEMA/SiO_2 for Pb^{2+} ion was a spontaneous process driven by entropy, and raising the temperature favored the adsorption process, which was consistent with the findings in the literature [26,36,37]. The entropy increased because the water molecules were replaced by hydroximic acid groups and released as free molecules from hydration ions originally combined with Pb^{2+} ions after SHA-PHEMA/SiO_2 chelating with Pb^{2+} ion. As a result, the number of particles in the system increases dramatically, resulting in the increase of entropy.

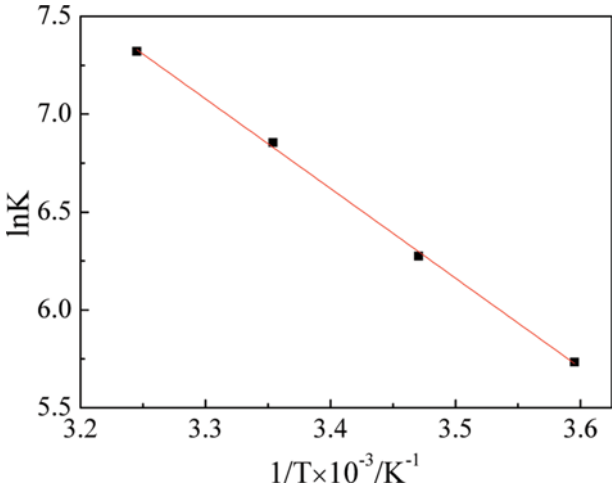

Fig. 14. Relationship between ln K and 1/T.

Table 4. Thermodynamics parameters for adsorption of Pb^{2+} ion on SHA-PHEMA/SiO_2

T/K	ΔG/(kJ·mol^{-1})	ΔH/(kJ·mol^{-1})	ΔS/(J·mol^{-1}·k^{-1})
278	−13.26	38.08	184.59
288	−15.03	38.08	184.34
298	−16.99	38.08	184.74
308	−18.76	38.08	184.46

6. Dynamic Adsorption and Elution Curves

Fig. 15 shows the dynamic adsorption curve of SHA-PHEMA/SiO_2 for Pb^{2+} ion. When the Pb^{2+} ion solution passed through the column packed with SHA-PHEMA/SiO_2 particles, the leak occurred at 44 BV, and the concentration of the effluent at 62 BV was the

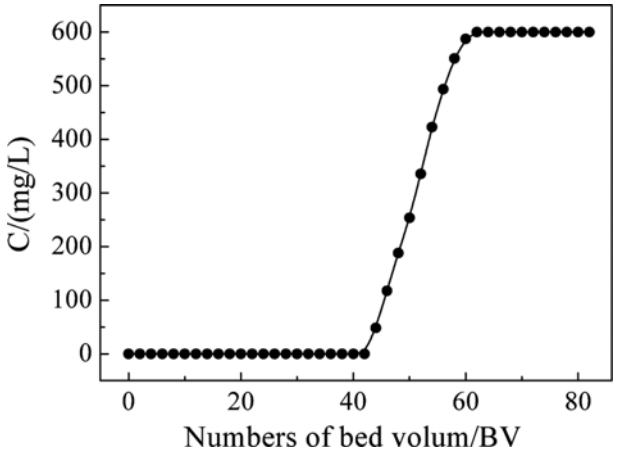

Fig. 15. Breakthrough curve of Pb^{2+} ion on SHA-PHEMA/SiO_2 column (T: 23 °C).

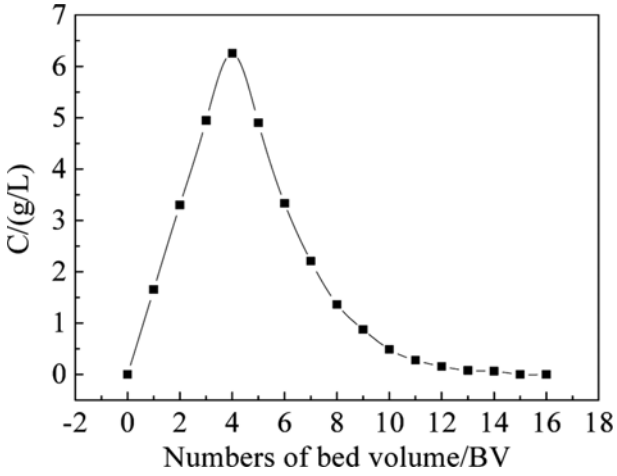

Fig. 16. Elution curves of Pb^{2+} ion from SHA-PHEMA/SiO_2 (T: 23 °C).

same as the initial concentration, indicating that the adsorption reached saturation point. The leak adsorption amount was calculated to be 46.97 mg/g, and the saturated adsorption amount was 53.58 mg/g. The dynamic adsorption amount was also high and similar to the static adsorption amount.

To reveal the actual application value of SHA-PHEMA/SiO_2, its desorption property was explored using hydrochloric acid solution with a concentration of 0.1 mol/L as the eluent with a rate of 1 BV/h flowing upstream through the column of SHA-PHEMA/SiO_2 saturated adsorption Pb^{2+} ion.

Fig. 16 presents the elution curve of Pb^{2+} ion from SHA-PHEMA/SiO_2. The shape of the desorption curve is cuspate and without tailing, indicating the fine elution of Pb^{2+} ion from SHA-PHEMA/SiO_2. The calculation results show that Pb^{2+} ion was eluted from SHA-PHEMA/SiO_2 column with desorption ratios of 96.2% and 99.5% within 9 BV and 13 BV, respectively. The result demonstrates that SHA-PHEMA/SiO_2 possessed remarkable elution property for Pb^{2+} ion, that is, the novel composite chelating material SHA-PHEMA/SiO_2 has excellent reusability.

7. Reusability

The static adsorption-desorption cycle was repeated ten times using the same material to measure the reusability of the chelating adsorption material SHA-PHEMA/SiO_2. The adsorption-desorption cycle is illustrated in Fig. 17. The adsorption amount of SHA-PHEMA/SiO_2 for Pb^{2+} ion declined slightly with the increase in the number of cycles of reuse, indicating that SHA-PHEMA/SiO_2 has excellent reusability.

CONCLUSIONS

Chloromethylation reaction of SHA was performed successfully to obtain CMSHA. Subsequently, the nucleophilic substitution reaction of CMSHA with grafted particles PHEMA/SiO_2 was achieved smoothly, and the salicylhydroxamic acid-functionalized composite chelating adsorbing material SHA-PHEMA/SiO_2 was prepared. SHA-PHEMA/SiO_2 possesses strong chelating adsorption ability for Pb^{2+} ions. The pseudo-second-order kinetic model described the adsorption process better than the pseudo-first-order model did. The chemical adsorption process was driven by entropy, and the adsorption capacity increased with rising temperature. The adsorption behavior conformed to the Langmuir isotherm model and was a monomolecular adsorption. At approximately pH≤6, the chelating adsorption capacity of SHA-PHEMA/SiO_2 toward Pb^{2+} ions was enhanced with the increasing pH value of the medium. Moreover, SHA-PHEMA/SiO_2 had excellent elution property and reusability. This kind of functional composite particles would be a promising adsorbent for removing heavy metal ions from industrial wastewater.

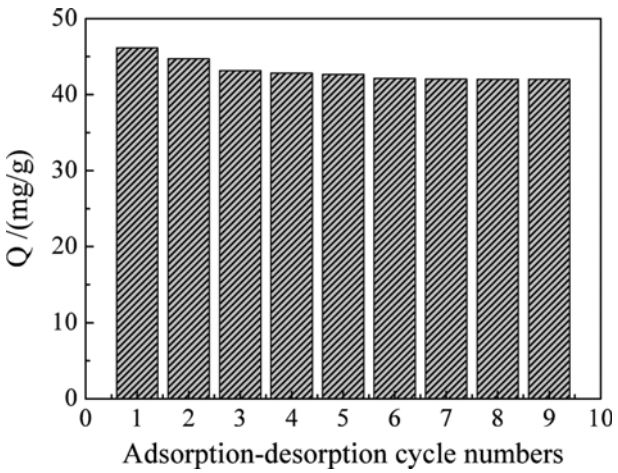

Fig. 17. Adsorption-desorption cycle of SHA-PHEMA/SiO_2 (T= 25 °C; t=2 h; pH=6; C_0=600 mg/L).

ACKNOWLEDGEMENTS

The authors gratefully acknowledge the National Science Foundation of China (No. 21307116), Natural Science Foundation of Province Shanxi of China (No. 2014011017-5), Program for Outstanding Innovative Teams of Higher Learning Institutions of Shanxi, and Fund Program for the Scientific Activities of Selected Returned Overseas Professionals in Shanxi Province for financial support of this work.

REFERENCES

1. O. Tatsuya, I. Sho, M. Hirofumi, O. Kaore and B. Yoshinari, *Sep. Purif. Technol.*, **114**, 11 (2013).
2. J. Zhang, B. J. Gao and J. H. Lu, *Acta Phys.-Chim. Sin.*, **25**, 532 (2009).
3. M. Y. Dang, H. M. Guo, Y. K. Tan and S. D. Bi, *Funct. Mater.*, **43**, 2616 (2012).
4. Y. Zhou, X. Yan and L. Q. Zhou, *CIESC J.*, **62**, 3288 (2011).
5. C. Park and J. T. Novak, *Water Res.*, **41**, 1679 (2007).
6. V. Mercedes, S. S. Sandra and V. R. María, *Inorganica Chimica Acta*, **393**, 24 (2012).
7. F. Rozada, M. Otero, A. Morán and A. I. García, *Bioresour. Technol.*, **99**, 6332 (2008).
8. L. F. Koong, K. F. Lam, J. Barford and M. Gordon, *Colloid Interface Sci.*, **395**, 230 (2013).
9. A. Abbas, S. Mohammad and B. Hasan, *J. Hazard. Mater.*, **181**, 836 (2010).
10. J. P. Wang, X. X. Ma, G. Z. Fang, M. F. Pan, X. K. Ye and S. Wang, *J. Hazard. Mater.*, **186**, 1985 (2011).
11. A. M. Donia, A. A. Atia and F. I. Abouzayed, *Chem. Eng. J.*, **191**, 22 (2012).
12. Y. W. Li, J. R. Li, L. F. Wang, B. Y. Zhou, Q. Chen and X. H. Bu, *J. Mater. Chem. A*, **1**, 495 (2013).
13. B. J. Gao, X. C. Gao and Y. B. Li, *Chem. Eng. J.*, **158**, 542 (2010).
14. J. Song, H. Kong and J. Jang, *J. Colloid Interface Sci.*, **359**, 505 (2011).
15. G M. Jiang, B. J. Gao, W. M. Xu and X. H. Wang, *Acta Phys.-Chim. Sin.*, **27**, 1474 (2011).
16. Q. J. Lei, G. Z. Zhang, B. J. Gao, F. Q. An, X. Dai, M. Wang and J. F. Gao, *Polym. Mater. Sci. Eng.*, **29**, 78 (2013).
17. J. Xu, S. J. Franklin, D. W. Whisenhun and K. N. Raymond, *J. Am. Chem. Soc.*, **117**, 7245 (1995).
18. W. Zeng, G. Y. Zeng and S. Y. Qin, *Chin. J. Org. Chem.*, **23**, 1213 (2003).

19. L. P. Che, Y. F. Yu, J. X. Pang, J. Z. Yuan and F. G. Zhang, *Rare Earths*, **25**, 49 (2004).
20. B. Yan, C. C. Zhou, X. R. Zhao and X. C. Ren, *Light Metals*, **4**, 7 (2011).
21. L. P. Jia, X. K. Che, Q. Zheng and L. Zhang, *Metal Mine*, **7**, 106 (2011).
22. W. G. Liu, B. Y. Wang, S. J. Dai, A. X. Ma and D. Z. Wei, *Non-Ferrous Mining Metallurgy*, **22**, 25 (2006).
23. H. Yang, S. Y. Qin and X. X. Lu, *Chin. Chem. Lett.*, **10**, 79 (1999).
24. H. B. Li, C. Qin, W. Liang, L. P. Wang, M. A. Hao, B. Jin, X. L. Liang and S. Y. Qin, *Mol. Catal.*, **23**, 62 (2009).
25. W. Zeng, J. Z. Li, H. B. Li and S. Y. Qin, *Chem. Res. Appl.*, **15**, 327 (2003).
26. M. Thomas, J. P. Gesson and S. Papot, *J. Org. Chem.*, **72**, 4262 (2007).
27. Y. L. Sheng, Y. F. Yang, B. J. Gao and Y. Zhu, *Acta Polym. Sin.*, **6**, 559 (2007).
28. X. H. Shi, R. X. Wang, B. J. Gao, C. P. Lei and Y. H. Li, *Polym. Mater. Sci. Eng.*, **31**, 139 (2015).
29. X. L. Fang, B. J. Gao, X. W. Huang, Y. Q. Zhang and L. R. Gu, *Acta Polym. Sin.*, **12**, 1472 (2012).
30. X. Xu, B. Y. Gao, W. Y. Wang, Q. Y. Yue, Y. Wang and S. Q. Ni, *Colloids Surf., B*, **70**, 46 (2009).
31. A. Khaled, A. E. Nemr, A. El-Silkaily and O. Abdelwahab, *J. Hazard. Mater.*, **165**, 100 (2009).
32. M. D. P. De Costa, W. A. P. A. Jayasinghe, *J. Photochem. Photobiol., A*, **162**, 591 (2004).
33. B. J. Gao, Y. C. Gao and Y. B. Li, *Chem. Eng. J.*, **158**, 542 (2010).
34. A. R. Cestari, E. F. S. Vieira and C. R. S. Mattos, *J. Chem. Thermodyn.*, **38**, 1092 (2006).
35. F. S. C. Anjos, E. F. S. Vieira and A. R. Cestari1, *Colloid Interface Sci.*, **253**, 243 (2002).
36. H. Chen and A. Q. Wang, *J. Hazard. Mater.*, **165**, 223 (2009).
37. I. Hatay, R. Gup and M. Ersöz, *J. Hazard. Mater.*, **150**, 546 (2008).